Radar range-polarization profile estimation using bispectrum-based reconstruction of naval object shape

Alexander V. Totsky, Anatoly V. Popov , Igor V. Kurbatov, Vladimir V. Lukin,
Jaakko Astola and Karen Egiazarian

The problem of range profile (RP) estimation for naval objects is considered. Based on the analysis of the received polarimetric signal at detector output, it is shown that it contains several components characterized by temporal and spatial non-stationarity. Two range profile estimation techniques are considered and compared. The former consists in conventional averaging received signal envelopes, while the second is based on bispectrum reconstruction of the received signal envelopes. X-band radar characteristics and the conditions of experimental measurement carrying out are presented. The analysis of the experimental results obtained for real radar data is performed for different polarization combinations and environment conditions (wind speed and sea state). The plots of RP estimations are represented and compared. They demonstrate the superiority of the bispectrum-based technique for RP estimation in the sense of better reconstruction of object shape and more efficient clutter suppression.

1. Introduction

Automatic target recognition (ATR) techniques using radar RP estimations are of ever-growing interest [1 – 6]. There is a variety of approaches to ATR problem such as optimal statistical pattern recognition using wide band and multi frequency radiation [1], the use of neural network-based classifiers [5], target polarization signatures [6], target shape reconstruction by bispectrum-based techniques [2 – 4], etc. Such variability of approaches deals with the following. First, there are many different factors affecting the quality of the obtained RPs and the performance of ATR methods. These factors are target rotation and translation during data acquisition, noise and/or clutter influence, heterogeneity of propagation channel, etc. Because of all this, the ATR is a very complicated task. Second, the performance of ATR systems depends upon the radar characteristics and operation principles, the effectiveness of signal processing techniques, the stability of RP characteristics (features), the effectiveness of the classifier.

This is why, considerable efforts are spent on improving ATR system performance at different stages. For example, wideband radars are used to provide high resolution RPs of targets and improve scatterer distribution estimations [1]. Bispectrum-based methods possess good immunity to RP translation and permit to quasi-coherently store several observations [2 – 4]. Some improvements to target recognition by its radar RP can be obtained by using target polarization signatures [6] that extend feature space.

Below we consider the task of RP estimation obtaining for naval objects. Although naval targets have relatively low velocities in comparison to aerial targets, the naval object RPs obtained by conventional radar signal processing methods still depend on target aspect angle and they are translation variant. Another peculiar feature that restricts naval object identification in maritime environment is the presence of sea clutter and radar echo interference caused by backscattering of electromagnetic waves from the surface of the sea. There are many scientific papers dealing with sea clutter (see, for example, [7]) that demonstrate the complicated and unstable nature of the statistical characteristics of the backscattered signal, which depend on random dynamic of sea clutter, grazing angle of observations, radar signal frequency and polarization. Because of this, it is usually rather

difficult to suppress sea clutter to separate naval object RP from sea interference.

The promising results of our previous investigations on bispectrum-based methods to reconstruct randomly shifted video signals [8] and preliminary analysis of experimental radar data provoked us to apply bispectrum-based approach to the problem of restoration of naval object radar portraits (RPs). It should be especially stressed, that in [8] the possibility of non-Gaussion interference suppression by bispectrum-based approach has been shown.

In this paper we consider the bispectrum-based approach to naval object RP reconstruction using experimental range naval object portraits obtained by X-band polarimetric radar for the cases of non-Gaussian sea clutter interference that usually can be described by log-normal, log-Weibull or K-distributed lows [7].

Despite the use of bispectrum analysis for RP estimation has been already presented for aerial targets recognition [2 – 4], application of bispectum-based RP reconstruction to naval object recognition has not been investigated yet. That is why, in this paper we are focusing on the problem of bispectrum-based RP reconstruction for a the naval object observed in the background of sea clutter.

The structure of this paper is the following. Conventional (averaging received signal envelopes) and bispectrum-based (bispectrum reconstruction of received signal envelopes) approaches in RP estimation are described and compared in Section 2. The characteristics of polarimetric radar and the results of experimental data analysis are presented in Section 3. Finally, the conclusions are given.

2. Problem statement

2.1. Conventional approach to radar range-polarization profile estimation by averaging received signal envelopes

Let us consider spatial-temporal model of received signals that correspond to reflections from a naval object and interference that is caused by sea surface backscattering. We assume that the dimensions of the object are significantly larger than wavelength. The relative location of transmitting-receiving on-land antenna, the backscattering area Ω that is limited by antenna beamwidth, the naval object and backscattering sea surface are shown in Fig.1. The plane of Cartesian coordinate system XOY is consisted with antenna aperture, and its origin is positioned onto aperture center. Total area Ω can be divided into a set of independent elementary surfaces $\Delta\boldsymbol{\theta}$ with reflection coefficients that are different for the metallic object and the sea surface. Assume that the antenna is fixed and its pattern maximum is oriented to the object effective reflection center $\boldsymbol{\theta_0}$. Define the coordinates of elements $\Delta\boldsymbol{\theta}$ of the area Ω by vector $\boldsymbol{\theta} = (\theta_x, \theta_y)$ with directive cosines θ_x, and θ_y.

Let the antenna irradiate narrow-band signal in the form of M RF impulse train with rectangular shape and without any carrier modulation. Write down the received signal $\dot{s}_{ik}(t)$ as

$$\dot{s}_{ik}(t) = \dot{S}_{ik}(t)\exp(j2\pi f_0 t), \qquad (1)$$

where $t \in [-T/2, T/2]$ denotes time; $i,k=\{H,V\}$ are the indices that correspond to horizontal and vertical polarization; $\dot{S}_{ik}(t - m\tau_p) = \begin{cases} 1, & \left|t - mT_r\right| \le \tau_{p/2} \\ 0, & \left|t - mT_r\right| > \tau_{p/2} \end{cases}$ is the complex envelope; τ_p denotes the pulse length; $T=T_rM$ is the total radar transmitting/processing time, T_r is the pulse repetition period; m=1,2,3,…,M defines the pulse index; f_0 is the central frequency, $f \in [f_0 - \Delta F/2, f_0 + \Delta F/2]$ where the bandwidth $\Delta F << f_0$; $j = \sqrt{-1}$.

During the time interval T the object position can change, its orientation and visibility can also vary. Because of this and the dynamic of maritime environment, to obtain a smooth estimation of the radar RP, the conventional techniques presume dividing time

interval T into N segments, and carrying out the averaging for N observed realizations (see, for example, [5]).

Assuming that additive noise (internal and background noise) is negligible, the n-th (n=1,2,…,N) echo signal realization (the n-th temporal scan) observed at the amplitude detector output is

$$S_{ik}^{(n)}(l\Delta t) = \mathrm{Re}\{\int_{\Omega} \dot{F}(\theta)\dot{\varepsilon}_{ik}^{(n)}(\theta, l\Delta t)\dot{S}[l(\Delta t + T_r) - \tau(\theta)]d\theta\}, \quad (2)$$

where $\dot{F}(\theta)$ is the complex antenna pattern; $\dot{\varepsilon}_{ik}^{(n)}(\theta)$ is the n-th relative (normalized for surface unit equal to 1 m^2) complex backscattering coefficient; $\tau(\theta)=2R(\theta)/c$ denotes the time delay; $R(\theta)$ and c are the slant range and light speed, respectively; l=1,2,…,L is the time pulse index; $L=M/N$ is the total sample number for one scan; Δt is the pulse repetition period corresponding to the range bin $\Delta R=c\Delta t$.

Equation (2) is valid under spatial-temporal band-limitedness, $2\Delta F/f_0<\lambda_0/D$, $\lambda_0=c/f_0$, D denotes the antenna aperture.

The coefficients $\dot{\varepsilon}_{ik}^{(n)}(\theta, l\Delta t)$ in (2) can be defined by the sum of random reflection components $\dot{\varepsilon}_{T\,ik}^{(n)}(\theta, \Delta t)$ corresponding to the echoes from the elementary surfaces $\Delta\theta$ of the randomly moving object and the random component $\dot{\varepsilon}_{S\,ik}^{(n)}(\theta, l\Delta t)$ caused by sea backscattering. These two components are statistically independent because they result from principally different spatial and temporal origin. Hence, $\dot{\varepsilon}_{ik}^{(n)}(\theta, l\Delta t)$ can be expressed as

$$\dot{\varepsilon}_{ik}^{(n)}(\theta, l\Delta t) = \dot{\varepsilon}_{T\,ik}^{(n)}(\theta, l\Delta t) + \dot{\varepsilon}_{S\,ik}^{(n)}(\theta, l\Delta t), \quad (3)$$

where the first term can be determined by signal polarization matrix with coefficients $\dot{\varepsilon}_{T\,ik}^{(n)}(\theta, \Delta t) = \left|\dot{\varepsilon}_{T\,ik}^{(n)}(\theta, \Delta t)\right| \exp[j\xi_{T\,ik}^{(n)}(\theta, \Delta t)]$ and the second term is determined by interference (sea backscattering) polarization matrix with random coefficients

$$\dot{\varepsilon}_{S\,ik}^{(n)}(\theta, \Delta t) = \left|\dot{\varepsilon}_{S\,ik}^{(n)}(\theta, \Delta t)\right| \exp[j\xi_{S\,ik}^{(n)}(\theta, \Delta t)].$$

Note that the term $\dot{\varepsilon}_{S\,ik}^{(n)}(\theta, \Delta t)$ usually includes the contributions caused by the following wave propagation paths:

- antenna-sea surface-antenna;
- antenna-sea surface-object-antenna;
- antenna-object-sea surface-antenna;
- antenna-sea surface-object-sea surface-antenna.

Conventional RP estimate is obtained using the averaging for N realizations. Due to statistical independence of signal and interference, it can be written as

$$\hat{S}_{ik}(l\Delta t) = \left\langle S_{ik}^{(n)}(l\Delta t)\right\rangle = \left\langle \tilde{S}_T^{(n)}[l\Delta t - \bar{\tau}_T^{(n)}]\right\rangle + \left\langle \tilde{S}_S^{(n)}[l\Delta t - \bar{\tau}_S^{(n)}]\right\rangle, \quad (4)$$

where $\tilde{S}_T^{(n)}(...)$ and $\tilde{S}_S^{(n)}(...)$ are the n-th echo envelopes smoothed by antenna pattern and corresponding to the object reflections and to the sea backscattering, respectively; $\bar{\tau}_T^{(n)}$ denotes the time lag integrated for all object reflecting elements during the n-th scan; $\bar{\tau}_S^{(n)}$ is the time lag integrated for all sea backscattering elements during the n-th scan; <…> denotes the averaging for N realizations (for N observed scans). Both $\bar{\tau}_T^{(n)}$ and $\bar{\tau}_S^{(n)}$ are random values that alternate from one realization to another.

The analysis of the relationships (2 – 4) reveals that:

1) The antenna integrates the multiple reflections and interference into common temporal signal due to influence of $\dot{F}(\theta)$ cut-off property. As the result of random object motions on the sea surface, the object response is a fluctuation process that changes from one scan to another and it has specific probability density function (pdf).

2) The different propagation paths lead to different time lags $\bar{\tau}_T^{(n)}$ and $\bar{\tau}_S^{(n)}$ in received signals (4), and these lags vary randomly from one scan to another.

The object and sea responses are independent processes for which the corresponding pdf and correlation intervals differ from each other. The correlation intervals for processes that correspond to reflections from sea surface elements are comparable to one scan processing time [6]. Therefore, the response from the sea is rapidly fluctuating process that changes from one scan to another. Thus, the time varying sea echo responses that usually overlap with the object response can destroy the estimate (4).

2.2. Bispectrum-based approach to radar RP estimation

Bispectrum-based RP estimation techniques have the following two advantages: 1) possibility to preserve Fourier spectrum phase information; 2) insensitivity to processed signal time shifts.

Bispectrum estimation $\hat{\dot{B}}(p,q)$ of (4) can be derived by direct technique [9] and written as

$$\hat{\dot{B}}(p,q)=\left|\hat{\dot{B}}(p,q)\right|e^{j\hat{\gamma}(p,q)}=\left\langle \dot{X}^{(n)}(p)\dot{X}^{(n)}(q)\dot{X}^{(n)*}(p+q)\right\rangle, \quad (5)$$

where $\left|\hat{\dot{B}}(p,q)\right|$ and $\hat{\gamma}(p,q)$ are the magnitude and phase bispectrum estimations, respectively; p=1,2,…,L and q=1,2,…,L are the independent frequency indices; $\dot{X}^{(n)}(...)$ is the direct Fourier transform of (2): $\dot{X}^{(n)}(p)=\dot{S}_T^{(n)}(p)e^{j2\pi\tau_T^{(n)}p}+\dot{S}_S^{(n)}(p)e^{j2\pi\tau_S^{(n)}p}$; $\dot{S}_T^{(n)}(p)$ and $\dot{S}_S^{(n)}(p)$ are the Fourier transforms of the object $\tilde{S}_T^{(n)}(...)$ and sea $\tilde{S}_S^{(n)}(...)$ responses in (4), respectively; * denotes complex conjugation.

Expression (5) can be rewritten on basis of (4) with regard to statistical independence of the object and sea radar responses. Then, due to the shift invariance property of bispectrum, one gets

$$\begin{aligned}\hat{\dot{B}}(p,q)=\hat{\dot{B}}_T(p,q)&+\left\langle \dot{S}_T^{(n)}(p)\dot{S}_T^{(n)}(q)e^{-j2\pi\tau_T^{(n)}(p+q)}\right\rangle\left\langle \dot{S}_S^{(n)*}(p+q)e^{j2\pi\tau_S^{(n)}(p+q)}\right\rangle+\\&\left\langle \dot{S}_T^{(n)}(p)\dot{S}_T^{(n)*}(p+q)e^{j2\pi\tau_T^{(n)}q}\right\rangle\left\langle \dot{S}_S^{(n)}(q)e^{-j2\pi\tau_S^{(n)}q}\right\rangle+\\&\left\langle \dot{S}_T^{(n)}(q)\dot{S}_T^{(n)*}(p+q)e^{j2\pi\tau_T^{(n)}q}\right\rangle\left\langle \dot{S}_S^{(n)}(p)e^{-j2\pi\tau_S^{(n)}p}\right\rangle+\\&\left\langle \dot{S}_T^{(n)}(p)e^{-j2\pi\tau_T^{(n)}p}\right\rangle\left\langle \dot{S}_S^{(n)}(q)\dot{S}_S^{(n)*}(p+q)e^{j2\pi\tau_S^{(n)}p}\right\rangle+\\&\left\langle \dot{S}_T^{(n)}(q)e^{-j2\pi\tau_T^{(n)}q}\right\rangle\left\langle \dot{S}_S^{(n)}(p)\dot{S}_S^{(n)*}(p+q)e^{j2\pi\tau_S^{(n)}q}\right\rangle+\\&\left\langle \dot{S}_T^{(n)*}(p+q)e^{j2\pi\tau_T^{(n)}(p+q)}\right\rangle\left\langle \dot{S}_S^{(n)}(p)\dot{S}_S^{(n)}(q)e^{-j2\pi\tau_S^{(n)}(p+q)}\right\rangle+\\&\hat{\dot{B}}_S(p,q)\end{aligned} \quad . \quad (6)$$

The first term in formula (6) $\hat{\dot{B}}_T(p,q)=\left\langle \dot{S}_T^{(n)}(p)\dot{S}_T^{(n)}(q)\dot{S}_T^{(n)*}(p+q)\right\rangle$ is the original RP object bispectrum. The other terms in (6) are the interference terms that degrade the bispectrum estimation of object RP. Theoretically, sufficiently good accuracy of $\hat{\dot{B}}_T(p,q)$ can be obtained under traditional assumptions that interference is zero-mean, and its pdf is close to symmetric [9,10]. The case of sea clutter with non-zero mean and with long tail pdfs needs to be studied and this problem is one of the subjects of our experimental investigation in this paper.

Finally, bispectrum-based object RP estimate can be represented as the following inverse Fourier transform (IFT)

$$\hat{S}_{range}(l)=\left|IFT\left\{\left|\hat{\dot{S}}_{bisp}(r)\right|e^{j\hat{\varphi}_{bisp}(r)}\right\}\right|,\ r=1,2,\ldots,L \quad (7)$$

where the magnitude $\left|\hat{\dot{S}}_{bisp}(r)\right|$ and phase $\hat{\varphi}_{bisp}(r)$ object RP Fourier spectrum estimations can be recovered from (6) by algorithms [10]

$$\hat{\varphi}_{bisp}(p+q)=\hat{\varphi}_{bisp}(p)+\hat{\varphi}_{bisp}(q)+\hat{\gamma}(p,q), \quad (8)$$

$$\left|\hat{\dot{S}}_{bisp}(p+q)\right|=\frac{\left|\hat{\dot{B}}(p,q)\right|}{\left|\hat{\dot{S}}_{bisp}(p)\right|\left|\hat{\dot{S}}_{bisp}(q)\right|}. \quad (9)$$

3. Discussion of Experimental Results

3.1. Description of experimental measurement conditions

Experimental investigations were carried out in summer period using on-land X-band polarimetric radar with f_0=9.370 MHz. The fixed antenna was located at the height of y_0=8 m over sea level (see Fig. 1) on the Black Sea shore in Crimea.

The radar basic characteristics are the following:

- the antenna beamwidth is 3.0^0 in both azimuth and elevation;
- the transmitted peak power is 10 kW;
- the pulsewidth is 3 μs;
- the pulse repetition frequency is 400 Hz for the total set of polarization combinations, i.e. for HH, HV, VH and VV polarizations (the first letter corresponds to transmitted wave polarization while the second one denotes the received signal polarization), thus, it is 100 Hz for each polarization component combination;
- two synchronous receiving channels for H and V polarization were employed; the separation of the channels is over 30 dB;
- the dynamic range of receiver is not less than 120 dB;
- the ADC capacity is 10 bits;
- the access time is 50 ns;
- the sample pulse step is equal to 250 ns that corresponds to the range bin of 75m.

After passing through analog IF amplifier and amplitude detector, the received signals were digitized and recorded in the memory block. The IF amplifier and detector characteristics were close to linear. The sampled data were recorded in the form of scans (realizations) with L=32 samples for each HH, HV, VH and VV polarization. The scan duration for each polarization was equal to 320 ms.

The antenna was pointed to the object with the aid of video camera fixed to the antenna. The anchored metallic buoy served as the naval object. Its size was considerably smaller than the range bin. The object radar echoes were recorded under small grazing angles of about 0.4^0.

3.2. Discussion of experimental results

In this section we compare the bispectrum-based RP reconstruction (see formulas (5 – 9)) with RP estimations obtained by conventional direct averaging (4). The number of recorded scans for each polarization was N=256.

Fig.2 shows consecutive scans for HH polarization, i.e. normalized range profiles (NRP) as the function of range sample index l. The slant range to buoy was R=1500 m and the buoy range position approximately corresponds to the index 26. The total duration of 6 observed scans equals to 6x320ms=1920ms. Note, that *random* buoy motion on sea waves as well as *random* changes of the electromagnetic wave reflection angles can be expected to develop during this sufficiently long observation time interval. Hence, the behavior of the object $\dot{\varepsilon}^{(n)}_{T\,ik}(\theta,\Delta t)$ and sea $\dot{\varepsilon}^{(n)}_{S\,ik}(\theta,l\Delta t)$ reflection components in (3) were random during every observed scan.

As seen from Fig.2, the scan fragments corresponding to buoy location and to sea clutter have random nature and their appearance considerably changes from scan to scan. For some scans the object is

not visible (e.g., for scan #2). Though the object RP should appear itself as single peak because its size is much smaller than range bin, the object response shape is considerably distorted. Due to interference, several peaks are observed in the neighborhood of the index 26 – see the scans ##3,4,5,6. Such RP distortions prevent object classification.

To improve accuracy, one can simply average the scans for N realizations (see (4)). The averaged NRPs obtained for different polarizations are shown in Figures 3 – 8. The Figures 3 – 5 correspond to irregular sea waves and absence of wind. The Figures 6 – 8 correspond to sea state of 2…2,5 and the wind speed of 7…10 m/s.

As seen from Figures 3 – 5, when the sea backscattering is low, the NRPs for different polarizations are considerably distorted. The averaged object NRPs are spread and their width at the half-amplitude level varies from approximately 300 m (see the Figures 4 and 5) to 450 m (see Fig.3). These values are sufficiently larger than the range bin 75 m that can be expected as the object response width.

This effect appears due to sea clutter and the influence of interference from several electromagnetic wave propagation paths (see Section 2). The effect can be also partly induced by the random motion of the naval object and averaging of the randomly shifted object responses according to (4).

The sea clutter level observed in Figures 3 – 5 depends on polarization and its maximum varies from approximately – 6 dB (see Figures 4 and 5) to – 13 dB (see Fig.3).

With wind present and the sea state 2…2,5 (see Figures 6 – 8), the object RP width at the half-amplitude level varies approximately between 900 m and 300 m. In this case, sea clutter level varies approximately from –13 dB (see Figures 6 and 8) to –8 dB (see Fig.7).

Thus, analysis of the NRPs shown in the Figures 3 – 9 permits to note that:

- every observed object response shape is distorted due to the averaging of the set of randomly shifted received object signal envelopes (see Fig.2);
- sea clutter level is sufficiently high that can mask the object response in some cases (see, for example, Fig.6).

Consequently, conventional RP estimation technique based on the averaging received signal envelopes has low range resolution and low robustness to sea clutter.

The bispectrum-based NRP estimates reconstructed by algorithm (7 – 9) are shown in Figures 9 – 14. The Figures 9 – 11 correspond to irregular sea waves and absence of wind. The Figures 12 – 14 correspond to sea state of 2…2,5 and the wind speed of 7…10 m/s. Note, that due to bispectrum shift invariance these NRPs are centered with respect to the NRP center of gravity (index 16 corresponds to the object location in Figures 9 – 14).

With no wind, the RP width at the half-amplitude level equals approximately to 150 m and the sea clutter levels have the values –20 dB (Fig.10), –24 dB (Fig.9) and –26 dB (Fig.11). The bispectrum-based technique performance slightly worsens in the case of sea state 2…2,5 and wind speed of 7…10 m/s (see Figures 12 – 14). The RP width is between 150 m (see Figures 13 and 14) and 450 m (Fig.12) and the sea clutter level becomes equal to –17 dB (Fig.12), –28 dB (Fig.13), and –26 dB (Fig.14).

In Tables 1 and 2 the summarizing of the key parameters of the RP estimates (range resolution and sea clutter level) for two considered techniques are shown.

Table 1. Results obtained for averaging received signal envelopes corresponding formula (4).

Absence of wind			Wind speed of 7…10 m/s		
HH	HV	VV	HH	HV	VV
NRP width at the half-amplitude level, m					
450	300	300	900	300	300
Sea clutter level, dB					
-13	-6	-6	-13	-8	-13

Table 2. Results obtained for bispectrum-based reconstruction of the received signal envelopes corresponding formulas (5 – 9).

Absence of wind			Wind speed of 7…10 m/s		
HH	HV	VV	HH	HV	VV
NRP width at the half-amplitude level, m					
150	150	150	450	150	150
Sea clutter level, dB					
-24	-20	-26	-17	-28	-26

As seen from Table 1, the range resolution is worse by from 2 to 12 times in comparison to the theoretical radar range bin of 75 m.

The results represented in Table 2 demonstrate the stability of the range resolution that is worse only by 2 times in comparison to the above mentioned theoretical radar range bin except the case of wind speed of 7…10 m/s and HH polarization.

The values of the sea clutter levels given in Tables 1 and 2 depend upon polarization type and sea state. As clearly seen from comparison the data contained in the Tables 1 and 2, bispectrum-based technique allows reducing sea clutter level from 11 dB (HH polarization) to 20 dB (VV polarization) in the case of absence of wind and from 4 dB (HH polarization) to 20 dB (HV polarization) in the case of wind speed of 7…10 m/s.

Thus, with the bispectrum-based technique the resolution of the naval object on the background of sea clutter increases markedly.

4. Conclusions

We have considered two approaches to RP estimation of the naval objects. These techniques are the averaging of the set of the observed radar scans and bispectrum reconstruction of RP. These techniques have been numerically investigated and compared using experimental X-band radar polarimetric data.

Experimental simulation results demonstrate the promising possibility of improving the resolution of a priori unknown naval object on the background of sea clutter by bispectrum-based reconstruction of radar RPs. This bispectrum-based approach does not require a priori knowledge about object and interference characteristics.

Experimental results have demonstrated sea clutter suppression and good naval object resolution. These results have been achieved for low resolution, polarimetric X-band radar for different sea states.

It should be especially noted, that the most bispectrum-based signal reconstruction approaches deal with additive interference with symmetric pdf. The results of our experimental investigations show the capability of bispectrum-based technique to suppress the sea clutter interference with long tail pdfs. The positive effect of sea clutter suppression needs to be studied more in detail for the cases of different sea states, grazing angles, radar resolutions, frequency bands, naval object sizes, etc.

The computational complexity was sufficiently low to permit real time data processing by Pentium-IV processor. To our opinion, the bispectrum-based technique of RP estimation is a promising way to increase naval object classification accuracy for practical implementation.

The results presented in this paper are by no means exhaustive and serve only to demonstrate the effectiveness of the bispectrum-based approach for improving the performance of the naval RP estimation system.

Further investigations will be focused on signal classification problem using the bispectrum-based techniques of naval object RP estimation for polarimetric data.

References

[1] *Shirman, Y.D., Gorshkov, S.A., Leshenko, S.A., Orlenko, V.M.*, Aerial target backscattering simulation and study of radar recognition, detection and tracking'. Proc. IEEE International Radar Conference, May 2000, Alexandria, USA, pp. 521 – 526.

[2] *Jouny, I., Garber, F.D., Moses, R.I.*, Radar target identification using the bispectrum: a comparative

study, IEEE Trans. on Aerospace and Electronic Systems, 1995, vol. 31, no. 1, pp. 69 – 77.

[3] *Zhang, X.D., Shi, Y., Bao, Z.*, A new feature vector using selected bispectra for signal classification with application in radar target recognition, IEEE Trans. on Signal Processing, 2001, vol. 49, no. 9, pp. 1875 – 1885.

[4] *Pei, B., Bao, Z., Xing, M.*, Logarithm bispectrum-based approach to radar range profile for automatic target recognition, The Journal of the Pattern Recognition Society, 2002, vol. 35**,** pp. 2643 – 2651.

[5] *Inggs, M.R., Robinson, A.D,* Ship target recognition using low resolution radar and neural networks, IEEE Trans. on Aerospace and Electronic Systems, 1999, vol. 35, no. 2, pp. 386 – 393.

[6] *Ponomarev, V.I., Fabi, R.P., Popov, A.V., Babakov, M.F.*, Detection and recognition of the targets by means of use the signal polarization properties'. Proceedings of SPIE, April 1999, Orlando, USA, pp. 283 – 291.

[7] *Sayama, S., Sekine, M.*, Log-normal, log-Weibull and K-distributed sea clutter, IEICE Trans. Commun., 2002, vol. E85-B, no. 7, pp. 1375 – 1381.

[8] *Totsky, A.V., Kurbatov, I.V., Lukin, V.V., Zelensky, A.A.*, Use of 2-D filtering of bispectrum estimations for 1-D signal reconstruction in mixed noise environment, Proc. International TICSP, Workshop on Spectral Methods and Multirate Signal Processing, SMMSP'02, September 2002, Toulouse, France, pp. 171 – 178.

[9] *Nikias, C.L., Raghuveer, M.R.*, Bispectral estimation: A digital signal processing framework, Proc. IEEE, 1987, vol. 75, no. 7, pp. 869-891.

[10] *Bartelt, H., Lohmann, A.W., Wirnitzer, B.*, Phase and amplitude recovery from bispectra, Applied Optics, September 1984, vol. 23, pp. 3121 – 3129.

Alexander Totsky was born in 1952 in Kharkov, Ukraine. He graduated in 1974 from the Radio Physics Faculty, Kharkov State University, Kharkov, Ukraine, and received the Diploma in radio physics and electronics. From 1974 to 1977, he was with Research Institute for Physics and Technics, Sukhumi, Georgia. In 1981, 1987, he received the Candidate of Technical Science degree and Associate Professor Diploma from the Kharkov Aviation Institute, respectively. Since 1977, he has been with the Department of Transmitters, Receivers, and Signal Processing of the Faculty of Radio Electronic Systems of National Aerospace University, Kharkov, Ukraine. In the academic years 1986/1987, he was for 10 months a visiting Researcher at Palacky University, Olomouc, Czechoslovakia. Since 2002, he has been in cooperation with Tampere University of Technology and Tampere International Center for Signal Processing. His research interests include signal and image processing, bispectrum analysis, and signal reconstruction techniques.

Anatoly Popov was born in 1961 in Kharkov, Ukraine. He graduated in 1984 from the Faculty of Radioelectronic Systems, Kharkov Aviation Institute (now National Aerospace University), Kharkov, Ukraine, and received the Diploma in radio engineering He received Candidate of Technical Science Diploma in radio engineering in 1991. Now he is senior scientific researcher and senior lecturer of the National Aerospace University, Kharkov, Ukraine. His area of scientific interests includes radar systems of detection, selection and recognition; radar polarimetry, weather radars, remote sensing of a marine and earth surface.

Igor Kurbatov was born in 1971 in Kharkov, Ukraine. He graduated from the Kharkov Aviation Institute, Kharkov, Ukraine, in 1994, and received the Diploma of Computer Science. He is currently completing his work toward the degree of Candidate of Technical Science at the National Aerospace University, Kharkov, Ukraine, in bispectrum based signal and image reconstruction techniques. His

research interests include digital signal and image processing and their applications.

Vladimir Lukin was born in 1960 in Belarus (fSU). He graduated in 1983 from the Faculty of Radioelectronic Systems, Kharkov Aviation Institute (now National Aerospace University), Kharkov, Ukraine, and received the Diploma with Honours in radio engineering. Since then, he has been with the Department of Transmitters, Receivers, and Signal Processing of the same faculty. He received Candidate of Technical Science Diploma in radio engineering and Doctor of Technical Science Diploma in 1988 and 2003, respectively. In the academic years 1992/1993, he was for 5 months a visiting Researcher at Northen Jiaotong University (Beijing, China). Since 1995, he has been in cooperation with Tampere University of Technology (Institute of Signal Processing and TICSP). Since 1996, he has been in Program Committee of Nonlinear Image Processing Conference, SPIE Symposium Photonics West in San Jose, USA. Since 1989, he has been Vice-Chairman of the Department of Transmitters, Receivers, and Signal Processing. He has published more than 150 journal and conference papers in Ukraine, USA, Finland, Russia, and so forth. More than 70 of them are in English.

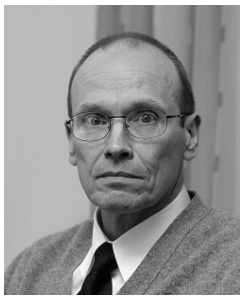

Jaakko Astola was born in Finland, in 1949. He received his B.S., M.S., Licentiate, and Ph.D. degrees in mathematics (specializing in error-correcting codes) from Turku University, Finland, in 1972, 1973, 1975 and 1978, respectively. From 1976 to 1977, he was in the Research Institute for Mathematical Sciences of Kyoto University, Kyoto, Japan. Between 1979 and 1987, he was with the Department of Information Technology, Lappeenranta University of Technology, Lappeenranta, Finland, holding various teaching positions in mathematics, applied mathematics, and computer science. In 1984, he worked as a visiting Scientist at Eindhoven University of Technology, the Nitherlands. From 1987 to 1992, he was an Associate Professor of applied mathematics at Tampere University, Tampere, Finland. From 1993, he has been Professor of Signal Processing and Director of Tampere International Center for Signal Processing, leading a group of about 60 scientists and was nominated Academy Professor by the Academy of Finland (2001 - 2006). His research interests include signal processing, coding theory, spectral techniques, and statistics. Dr. Astola is a fellow of the IEEE.

Karen Egiazarian was born in Yerevan, Armenia, in 1959. He received the M.Sc. degree in mathematics from Yerevan State University in 1981, and the Ph.D. Degree in physics and mathematics from Moscow M. V. Lomonosov State University in 1986. In 1994 he was awarded the degree of Doctor of Technology by Tampere University of Technology, Finland. He has been a Senior Researcher at the Department of Digital Signal Processing of the Institute of Information Problems and Automation, National Academy of Sciences of Armenia. He is currently a Professor at the Institute of Signal Processing, Tampere University of Technology. His research interests are in the areas of applied mathematics, digital logic, signal and image processing. He has published more than 200 articles in these areas, and is co-author (with S. Agaian and J. Astola) of the book "Binary Polynomial Transforms and Nonlinear Digital Filters", published by Marcel Dekker, Inc. in 1995, and three book chapters.

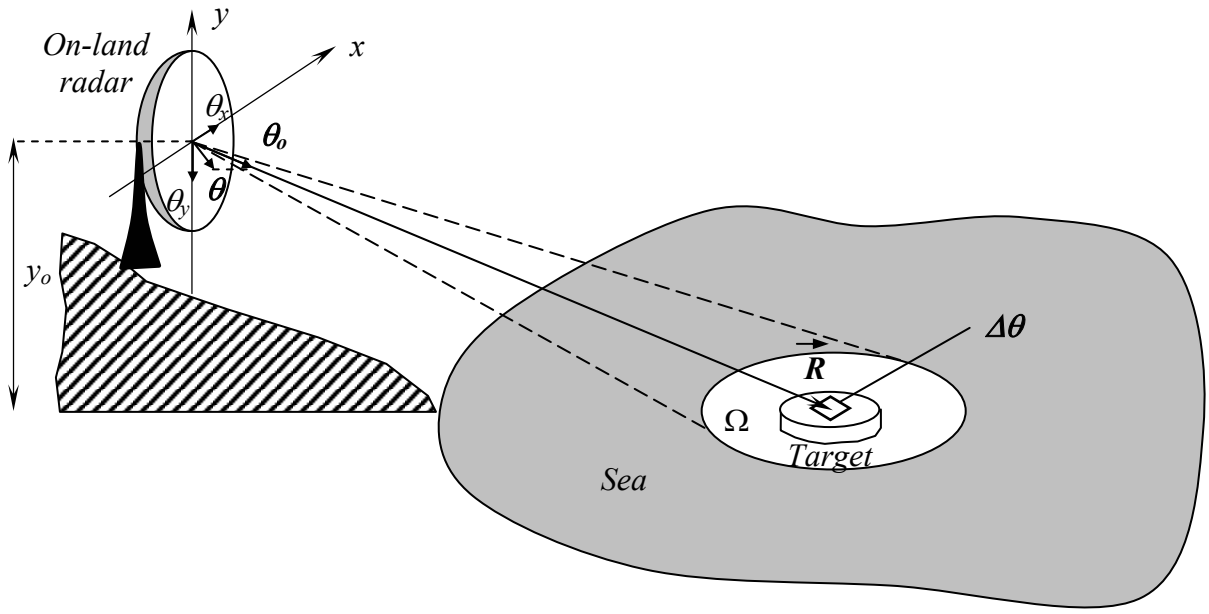

Figure 1. Geometric relationship of on-land radar and naval object.

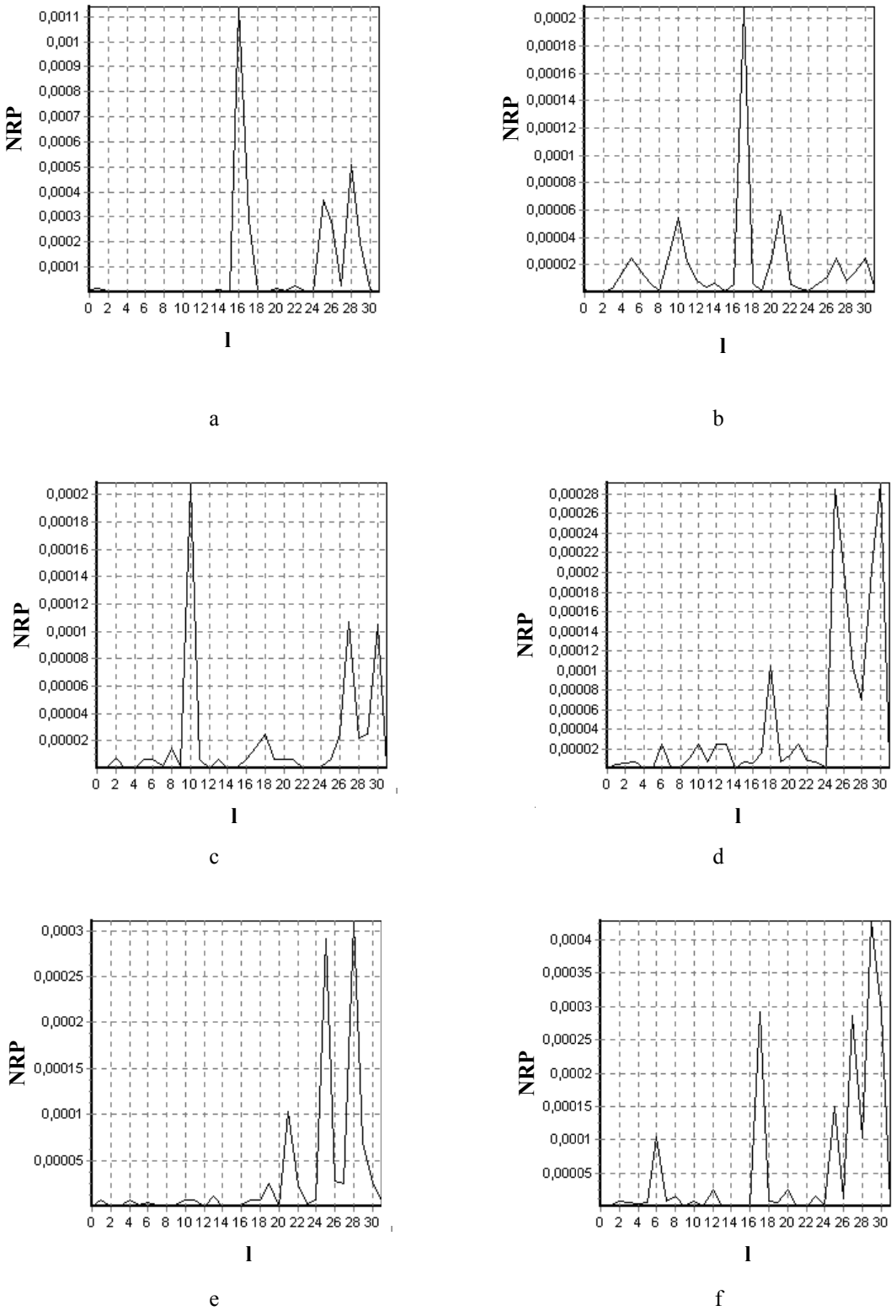

Figure 2. Consecutive scans: a) scan#1; b) scan#2; c) scan#3; d) scan#4; e) scan#5; f) scan#6.

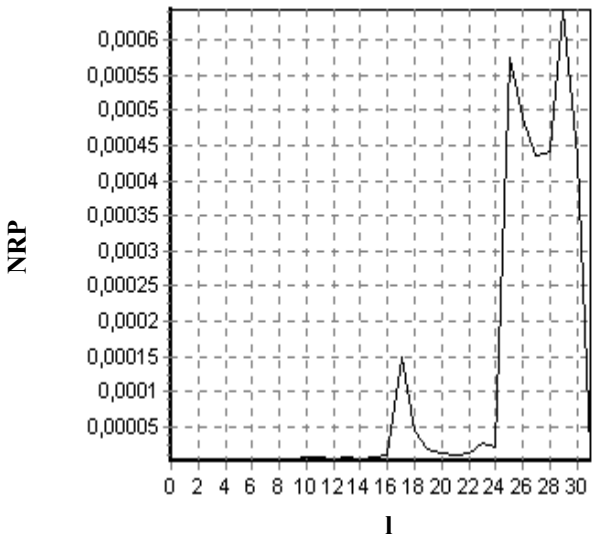

Figure 3. Averaged RP (HH, no wind).

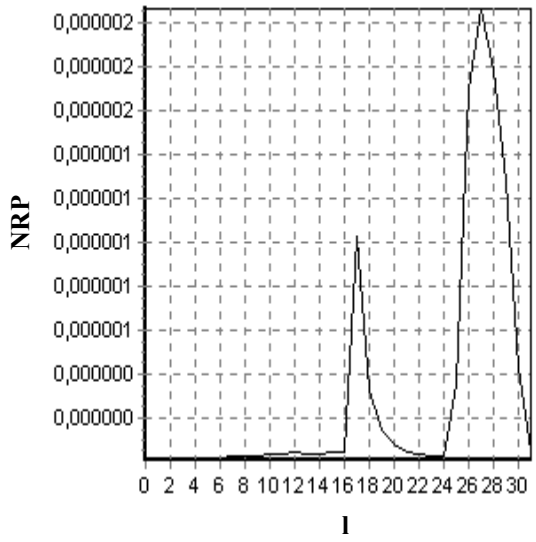

Figure 4. Averaged RP (HV, no wind).

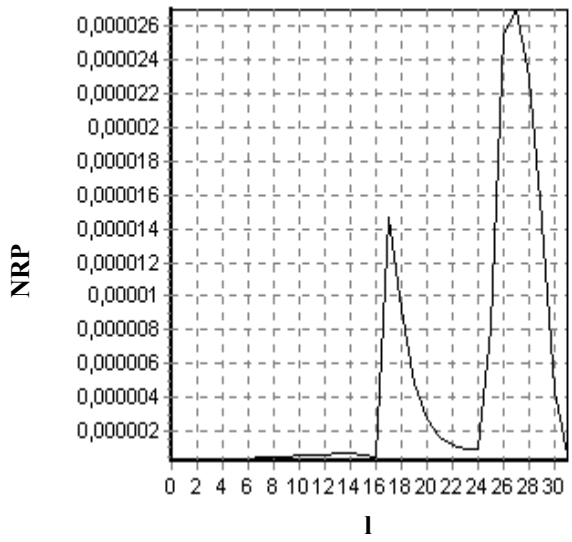

Figure 5. Averaged RP (VV, no wind).

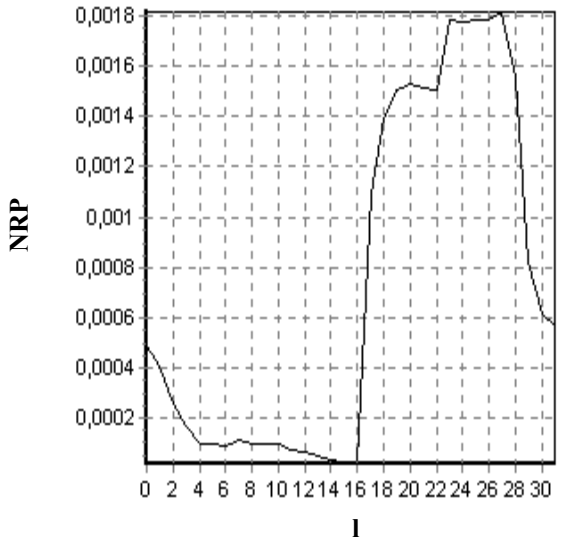

Figure 6. Averaged RP (HH, wind speed 7…10 m/s; sea state 2…2.5).

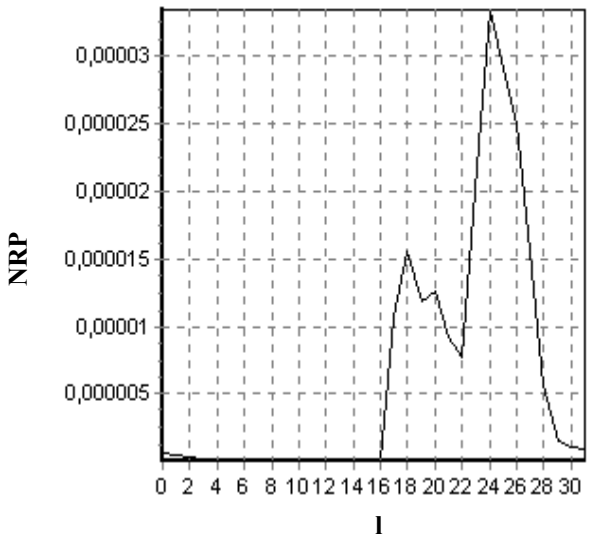

Figure 7. Averaged RP (HV, wind speed 7…10 m/s; sea state 2…2.5).

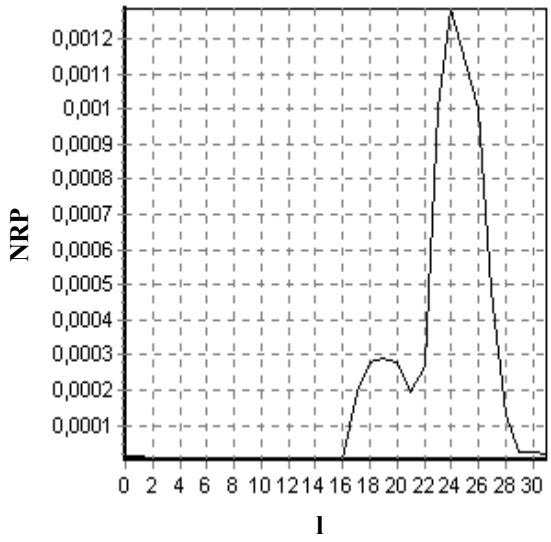

Figure 8. Averaged RP (VV, wind speed 7…10 m/s; sea state 2…2.5).

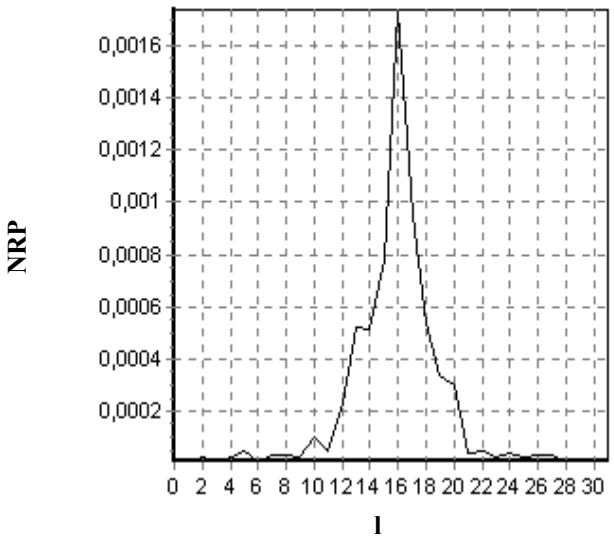

Figure 9. Bispectrum-based RP (HH, no wind).

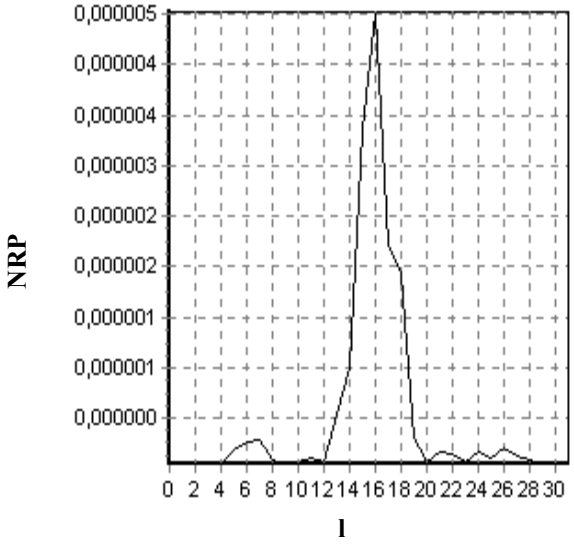

Figure 10. Bispectrum-based RP (HV, no wind).

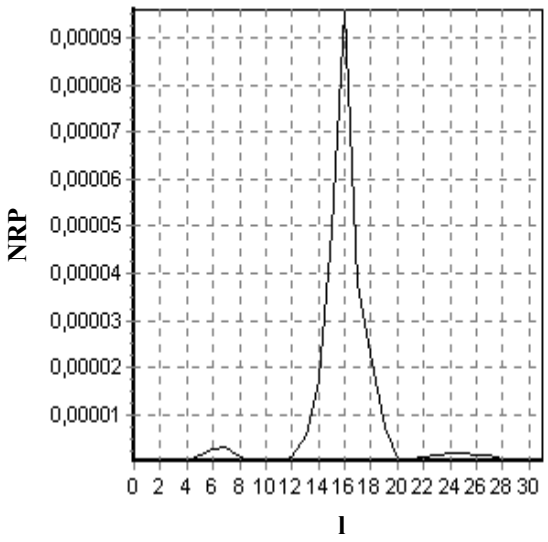

Figure 11. Bispectrum-based RP (VV, no wind).

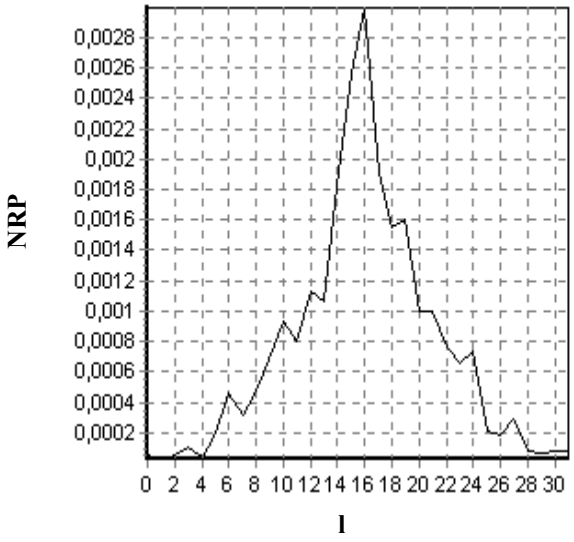

Figure 12. Bispectrum-based RP (HH, wind speed 7…10 m/s; sea state 2…2.5).

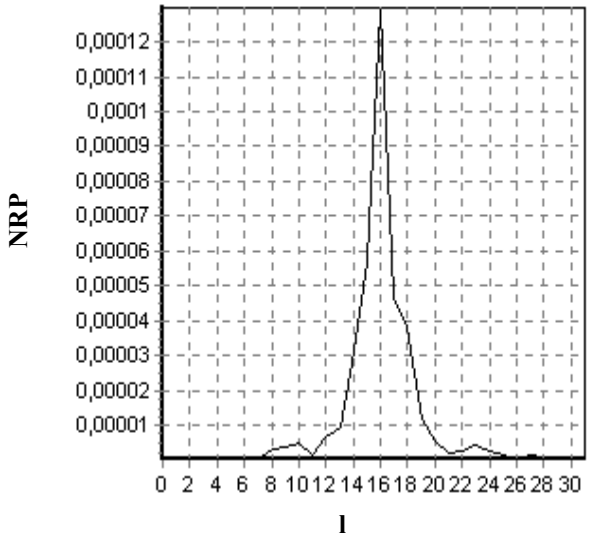

Figure 13. Bispectrum-based RP (HV, wind speed 7…10 m/s; sea state 2…2.5).

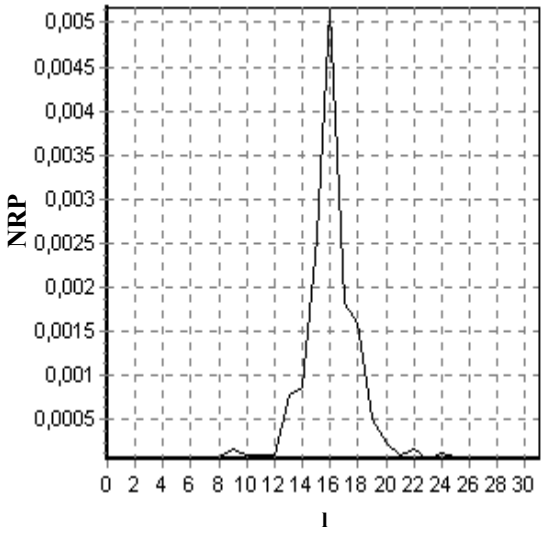

Figure 14. Bispectrum-based RP (VV, wind speed 7…10 m/s; sea state 2…2.5).